Video Article

# Analyzing Synaptic Modulation of *Drosophila melanogaster* Photoreceptors after Exposure to Prolonged Light

Atsushi Sugie[1,2,5], Christoph Möhl[3], Satoko Hakeda-Suzuki[4], Hideaki Matsui[1,2], Takashi Suzuki*[4], Gaia Tavosanis*[5]

[1]Department of Neuroscience of Disease, Center for Transdisciplinary Research, Niigata University

[2]Brain Research Institute, Niigata University

[3]Image and Data Analysis Facility, German Center for Neurodegenerative Diseases (DZNE)

[4]Graduate School of Life Science and Technology, Tokyo Institute of Technology (Titech)

[5]Dendrite Differentiation, German Center for Neurodegenerative Diseases (DZNE)

*These authors contributed equally

Correspondence to: Atsushi Sugie at atsushi.sugie@bri.niigata-u.ac.jp, Christoph Möhl at christoph.moehl@dzne.de

URL: https://www.jove.com/video/55176
DOI: doi:10.3791/55176

Keywords: Neuroscience, Issue 120, *Drosophila*, photoreceptor, synapse, active zone, Bruchpilot, light exposure

Date Published: 2/10/2017

Citation: Sugie, A., Möhl, C., Hakeda-Suzuki, S., Matsui, H., Suzuki, T., Tavosanis, G. Analyzing Synaptic Modulation of *Drosophila melanogaster* Photoreceptors after Exposure to Prolonged Light. *J. Vis. Exp.* (120), e55176, doi:10.3791/55176 (2017).

## Abstract

The nervous system has the remarkable ability to adapt and respond to various stimuli. This neural adjustment is largely achieved through plasticity at the synaptic level. The Active Zone (AZ) is the region at the presynaptic membrane that mediates neurotransmitter release and is composed of a dense collection of scaffold proteins. AZs of *Drosophila melanogaster* (*Drosophila*) photoreceptors undergo molecular remodeling after prolonged exposure to natural ambient light. Thus the level of neuronal activity can rearrange the molecular composition of the AZ and contribute to the regulation of the functional output.

Starting from the light exposure set-up preparation to the immunohistochemistry, this protocol details how to quantify the number, the spatial distribution, and the delocalization level of synaptic molecules at AZs in *Drosophila* photoreceptors. Using image analysis software, clusters of the GFP-fused AZ component Bruchpilot were identified for each R8 photoreceptor (R8) axon terminal. Detected Bruchpilot spots were automatically assigned to individual R8 axons. To calculate the distribution of spot frequency along the axon, we implemented a customized software plugin. Each axon's start-point and end-point were manually defined and the position of each Bruchpilot spot was projected onto the connecting line between start and end-point. Besides the number of Bruchpilot clusters, we also quantified the delocalization level of Bruchpilot-GFP within the clusters. These measurements reflect in detail the spatially resolved synaptic dynamics in a single neuron under different environmental conditions to stimuli.

## Video Link

The video component of this article can be found at https://www.jove.com/video/55176/

## Introduction

The modulation of synaptic function contributes to the remarkable ability of the nervous system to precisely respond or adapt to changing environmental stimuli. Adjusting the presynaptic vesicle release probability is one way of controlling synaptic strength[1]. Synaptic vesicle release takes place at the Active Zone (AZ), a specialized region of the presynaptic membrane[2]. The AZ is characterized by a cassette of specific proteins[3,4]. Most proteins contributing to AZ assembly are highly conserved in nematodes, insects and mammals[5]. Recent studies suggest that the level of neuronal activity regulates the molecular composition of the AZ, which in turn contributes to the regulation of the functional output both *in vitro* and *in vivo*[6,7,8]. We previously found that photoreceptor AZs undergo molecular remodeling in *Drosophila* after prolonged exposure to natural ambient light[9]. In this condition, we observed that the number of Bruchpilot (Brp)-positive AZs was reduced in the photoreceptor axons.

The Brp/CAST/ELKS family proteins are fundamental building blocks of AZs in vertebrate and invertebrate synapses[10]. In *Drosophila brp* mutants, evoked vesicle release is suppressed[11,12]. The 17 C-terminal amino acid residues of Brp are essential for synaptic vesicle clustering at the *Drosophila* Neuromuscular Junction (NMJ)[13,14]. These studies demonstrated the central role of this molecule in AZ organization and function. With a recently developed genetic tool, Synaptic Tagging with Recombination (STaR), Brp can be observed *in vivo* in specific cell types, at endogenous expression levels and at a single synapse resolution[15]. This tool makes it feasible to evaluate the endogenous dynamics of synapses quantitatively in the complex central nervous system.

There have been several studies including synapse quantifications based on data obtained from confocal microscopy. Synaptic alterations have been evaluated by measuring the length, the area, the volume, the density and counting the number based on sophisticated software applications. For instance, the freeware ImageJ provides a quantification method for total synaptic area and synaptic density measures at the *Drosophila* NMJ[16]. The number of colocalization sites of pre and postsynaptic markers have been quantified using the plugin "Puncta

 

Analyzer" available on the ImageJ software platform[17]. Alternatively, a multi-paradigm numerical computing environment based program, Synapse Detector (SynD), can automatically trace dendrites of neurons labeled with a fluorescent marker, and then quantifies the synaptic protein levels as a function of distance from the cell body[18]. The software Synaptic Puncta Analysis (SynPAnal), has been designed for the rapid analysis of 2D images of neurons acquired from confocal or fluorescent microscopy. The primary function of this software is the automatic and rapid quantification of density and intensity of protein puncta[19]. Recently, an automatic learning-based synapse detection algorithm has been generated for quantification of synaptic number in 3D[20], taking advantage of the 3D Visualization-Assisted Analysis (Vaa3D) software[21].

Commercial image analysis software are also powerful tools for synaptic quantifications. For instance, the fluorescently labeled neurotransmitter receptors or a presynaptic AZ component have been quantified in three dimensions with single-synapse resolution in *C. elegans*[22] or the *Drosophila* olfactory system[23,24], allowing hundreds of synapses to be rapidly characterized within a single sample.

Here, we present a method by a customized image analysis software plug-in implemented in a multi-paradigm numerical computing environment that allows to analyze semi-automatically multiple aspects of AZs, including their number, distribution and the level of enrichment of molecular components to the AZ. Thus, this complex analysis allowed us to evaluate the dynamics of synaptic components in axon terminals under different environmental conditions. We investigated the effect of light exposure on the output synapses of adult fly photoreceptors. The procedure is performed in three steps: 1) preparation for light exposure, 2) dissection, immunohistochemistry and confocal imaging, and 3) image analysis.

## Protocol

The experimental procedures described in this protocol involve exclusively work with *Drosophila* and are not subjected to animal welfare laws in Germany and Japan.

## 1. Light Exposure Conditions

1. Prepare flies that carry *sensless-flippase* (*sens-flp*) and *bruchpilot-FRT-STOP-FRT-gfp* (*brp-FSF-gfp*)[15] for visualizing Brp-GFP in photoreceptor R8 neurons (R8s). The genomic locus encoding *brp* within a Bacterial Artificial Chromosome (BAC) was modified to generate this *brp-FSF-gfp* construct. In the flies carrying this modified BAC the expression of Brp-GFP is under the control of the endogenous regulatory sequences, but limited to R8 photoreceptors after *sensless-flippase*-mediated removal of the FRT-STOP-FRT cassette[15]. Note that *sens-flp* rarely expresses flippase in R7s.
2. Keep the flies in a 12 h light/12 h dark cycle (LD) at 25 °C from the larva stage until eclosion (**Figure 1A**).
3. Collect the flies 0 - 6 h after eclosion and place them into a new vial containing fly food.
4. Set the vials into a transparent rack made of acrylic resin with three steps (a height of 41 cm, a base of 21 cm, a thickness of 4 cm and a height of 13 cm for each step) (**Figure 1B**).
5. Adjust the distance between the rack and a LED panel to provide the illumination with an average intensity of 1,000 lux using a digital light meter (**Figure 1C**).
6. Keep the flies for 1 - 3 d under one of the following conditions: constant darkness (DD), 12 h light/12 h dark cycle (LD), or constant light (LL) at 25 °C in a small incubator (**Figures 1A** and **1C**).

## 2. Dissection, Immunohistochemistry and Imaging

1. Dissect fly brains with forceps, fix them with 4% formaldehyde and immunostain with the primary antibody against Chaoptin (1:50) and a second antibody for visualization of photoreceptors based on previous experimental procedures[25]. Briefly:
    1. Prepare 0.1% Triton X-100 in PBS (0.1% PBT). This solution is used to improve antibody tissue penetration.
    2. Anesthetize flies on a $CO_2$ pad, sort out the correct genotype and transfer them to a petri dish filled with 0.1% PBT.
    3. Stick the forceps underneath the proboscis and pull off the right and left eyes respectively with the other forceps.
    4. Remove the proboscis and the trachea attached to the brain.
    5. Transfer the brain with the forceps into a 1.5 mL tube containing 150 µL of 0.1% PBT at RT.
    6. Within 10 min repeat from 2.1.3 - 2.1.5 to obtain as many brains as possible.
    7. Add 50 µL of 16% formaldehyde into the tube and mix by pipetting.
    8. Incubate the brains in fixative at room temperature for 50 min.
    9. Wash three times with 200 µL of 0.1% PBT with a micropipette, paying attention to leave the brains in the tube.
    10. After the last wash, remove the 0.1% PBT and add the primary antibody solution, prepared as follows: add to 196 µL of 0.3% PBT (0.3% Triton X-100 in PBS) 4 µL of anti-Chaoptin antibody (final dilution 1:50) for visualization of photoreceptors.
    11. Incubate the brains in the primary antibody solution at 4 °C O/N.
    12. Wash 3x with 200 µL of 0.1% PBT with a micropipette.
    13. After the last wash, remove the 0.1% PBT and add 200 µL of the 0.3% PBT containing a secondary antibody.
    14. Incubate it in the dark at 4 °C O/N.
    15. Wash three times with 200 µL of 0.1% PBT with a micropipette.
2. For mounting, put two small drops (2 µL each) of a mounting medium with a micropipette at the center of a microscope slide at approximately 2 cm distance from each other.
3. Place two coverslips, one onto each drop and leave a narrow gap between the coverslips of approximately 0.2 mm.
4. Place 15 µL of a mounting medium on top of the coverslip and add the brains with a micropipette into the mounting medium.
5. Under a dissecting microscope, position the brains with the ventral side up into the narrow gap between the two coverslips (**Figure 2**).
6. Place a coverslip on top and seal the edges of the coverslip using clear nail polish to fix the specimen (**Figure 2**).
7. Obtain images of the brains with a confocal microscope. Use a 63X oil immersion objective lens (1.4 N. A.) and a 2.6X digital zoom. Generate more than 20 optical sections of the second optic ganglion medulla with a step size of 0.5 µm.

## 3. Generation of the Spots, Surface Objects, Start-points and End-points

1. To quantify the number, the distribution and the delocalization level of Brp-GFP puncta, open the stack obtained by confocal microscopy in image analysis software and reconstitute 3D images (**Figure 3A**). Note that the step in this study was performed with Imaris.
2. Identify the Brp-GFP puncta by the spot detection module for each R8 axon terminal.
    1. Select "Add new Spots".
    2. Select "Segment only a Region of Interest" in the algorithm settings. Select an R8 axon terminal in the medulla manually.
    3. Select the source channel of the Brp-GFP signal.
    NOTE: The R7 and R8 photoreceptor axons were immunolabeled with anti-Chaoptin (**Figure 3A**). Only R8, though, contains Brp-GFP puncta and could thus be easily distinguished (**Figure 3A**). Further, the endpoint of R8 could be identified by the thinning of the anti-Chaoptin-positive axons at the entry point into the M3 medulla layer.
    4. Set the estimated XY diameter to 0.35 µm and check off "Background subtraction" in the spot detection.
    5. Select "Quality" in filter type and filter automatically. Then click finish.
    6. Repeat from 3.2.1 t- 3.2.5 for other R axons (**Figure 3B**).

3. To measure the delocalization level of Brp-GFP in R8 axons, generate surface objects with the "Surface" function for each axon (**Figure 3C**).
    1. Select "Add new Surfaces".
    2. Select "Segment only a Region of Interest" in the algorithm settings. Then select an R8 axon terminals in the medulla manually.
    3. Select the source channel of the photoreceptors.
    4. Check off "Smooth".
    5. Select "Absolute Intensity" in the threshold.
    6. Check "Enable". "Seed Points Diameter" is 0.5 µm.
    7. Select filter Type "Quality" and "Number of voxels", and then filter automatically.
    8. Go to "Edit" and delete the pieces of surfaces generated on other non-interesting axons.
    9. Repeat from 3.3.1 - 3.3.8 for other R axons (**Figure 3C**). Note some surface objects were interrupted because of the thinness and the weak signal in photoreceptors at M2 layer, but they were still considered as a single object from start to end points.

4. To identify the distribution of Brp-GFP puncta along each neuron in the medulla neuropil, define the start-point and end-point with the measurement point function (**Figure 3D**).
    1. Select "Add new Measurement Points". Then select "Edit" and select "Surface of Object" to intersect with the top of the surface objects.
    2. Put measurement points on top of surface objects of R axons in M1 layer in order. These are now defined as start-points (**Figure 3D**).
    3. Select "Add new Measurement Points". Then select "Edit" and select "Surface of Object" to intersect with the bottom of the surface objects.
    4. Put measurement points on the bottom of the surface objects of R axons in M3 layer in order. These are now defined as end-points (**Figure 3D**).

5. To subtract the background signal from the GFP channel, generate surface objects, spots, start-points and end-points for two R axons in M6 layer (**Figure 3E**).
    1. Select "Add new Surfaces".
    2. Select "Segment only a Region of Interest" in the algorithm settings. Then select a R7 axon terminal between M5 and M6 layer manually.
    3. Select the source channel of the photoreceptor.
    4. Check off "Smooth".
    5. Select "Absolute Intensity" in the threshold.
    6. Select filter Type "Quality" and "Number of voxels", then filter automatically.
    7. Select "Add new Spots".
    8. Select "Skip automatic creation, edit manually".
    9. Select "Center of Object" and add a spot in the inner area of the surface object generated from 3.5.1 - 3.5.6.
    10. Repeat from 3.5.1 - 3.5.9 for another R7 axon terminal.
    11. Select "Add new Measurement Points". Then select "Edit" and put measurement points on top of the two surface objects of the tip of the R7 axon terminal in M6 layer. These are now defined as start-points.
    12. Select "Add new Measurement Points". Then select "Edit" and put measurement points on the bottom of the two surface objects of the tip of the R7 axon terminal in M6 layer. These are now defined as end-points (**Figure 3E**).

## 4. Calculation of the Number of Spots, Distribution of the Spot Frequency and Level of Enrichment of Brp-GFP with a Customized Image Data Analysis Software

1. Copy the file "XtquantifySynapseSNR.m" and the "functions" folder into the Imaris XT matlab folder. Note that the calculation in this study was performed with a customized plugin implemented in Matlab. Download the plugin from the website (https://github.com/cmohl2013/synapse_trafo).
2. Open a dataset with n spots, n surfaces and 2 measurement point objects, each containing n measurement points (prepared from 3.1 - 3.4). The first measurement point object defines the start positions for all axons. The second measurement point object defines the end position of all axons. Both measurement point objects need to have the same number of measurement points (that is the number of axons).
3. Execute image processing>>CUSTOM>atsushis synapse detection Vs 6.
4. Check metadata and change pixel sizes in image analysis software in case it is not correct.
5. Select channel for the performance of the intensity analysis of spots regions and cytoplasmic regions (the channel with Brp-GFP).
6. Define the filename for exporting the results.

7. Define the number of bins and axon length in percent. Enter the number of bins as "10" and range of bins as "100%" (**Figures 4A** and **4B**).
8. Define the regions of the spots and the other cytoplasmic regions for the Brp-GFP delocalization analysis. Enter spots radius as "0.35 µm" and width of surrounding area as "50 µm". The spots radius defines the region for the puncta GFP signal (0.35 µm diameter, centered on one punctum). The width of surrounding area defines the region for the GFP signal in the cytoplasmic area (50 µm diameter, centered on the punctum, but including only R8 and excluding all spot areas in the cytoplasm) (**Figures 4A** and **4C**).
9. Wait until all neuron masks are processed and exported as PDF files (**Figures 4B** and **4C**) and a csv table for further analysis in a spreadsheet. The csv table includes the number of the spots, the average signal intensity in the "cytoplasmic area" and the maximum signal intensity in the "spot" in each bin for all R8 axons.
10. Open a dataset prepared in 3.5 for subtraction of the background signal.
11. Perform the image processing as described from 4.3 - 4.9.
12. Calculate the average of the total number and the distribution of the Brp-GFP puncta in a spreadsheet (**Figures 4D** and **4E**).
13. Calculate the average of the delocalization of Brp-GFP signal in a spreadsheet by the ratio of the average intensity in the "cytoplasmic area" divided by the maximum intensity in the "spot" subtracted by the average intensity in the background signal (**Figure 4F**).

## Representative Results

The compound eye of *Drosophila* comprises ~780 ommatidia, each containing eight types of photoreceptors (R1-8). R7 and R8 project their axons to the second optic ganglion, the medulla, where they form synapses in layers M6 and M3, respectively[26]. To investigate the effect of prolonged exposure to light on the molecular composition of photoreceptor R8 active zones, we took advantage of the STaR method[15]. Endogenous expression levels of Brp were fluorescently labeled by flipping out the stop codon in *brp-FSF-gfp* with a flippase expressed in R8 photoreceptors derived from the *sens-flp*. The flies were kept for 1 - 3 d after eclosion in LL, LD or DD for the same period of time at 25 °C (**Figure 1A**). To expose the flies to 1,000 Lux light, the flies were set into an acrylic resin rack (**Figure 1B**) and kept at the same distance from the LED light source in a small incubator (**Figure 1C**).

After immunostaining, dissected brains were placed into the narrow gap between two coverslips on a microscope slide with the ventral side of the brains facing upwards for visualization and quantification of the Brp-GFP puncta (**Figure 2**). The resulting Brp-GFP signal localized to distinct puncta within R8 in the medulla (**Figure 3A**).

To count the number and measure the distribution of Brp-GFP puncta, and to evaluate the delocalization level of Brp-GFP signal in R8s, a customized image analysis software plugin was developed in a multi-paradigm numerical computing environment[9,27]. At first, puncta were detected by a spot detection function for each R8 (**Figure 3B**). Subsequently, surfaces of each R8 were generated for evaluation of the delocalization level (**Figure 3C**). Finally, we defined start-points and end-points at the top of M1 layer and the bottom of M3 layer on each photoreceptor respectively to measure the AZ distribution (**Figure 3D**). Surface objects, spots, start-points and end-points for two R7 axon terminals in M6 layer were also generated to subtract the background signal from GFP channel (**Figure 3E**). The results of the number (**Figure 4D**), the distribution (**Figures 4A, 4B** and **4E**) and the delocalization level (**Figures 4A, 4C** and **4F**) are automatically calculated by the custom plug-in written in a multi-paradigm numerical computing environment. We found that the number of Brp discrete puncta was significantly reduced in R8 photoreceptors of flies kept in LL conditions (**Figures 4D** and **4E**). Additionally, we found that R8 synapses were distributed all along the axonal shaft from the M1 to the M3 layer, but the density was higher at the M1 and M3 layers (**Figure 4E**). The delocalization level of Brp-GFP was unchanged in all light conditions (**Figure 4F**). This is in contrast to the localization of a fluorescently tagged short version of Brp (Brp-short-cherry)[28], which, as we previously reported[9] becomes clearly diffused in LL (**Figure 4G**). We suggested that the delocalized Brp-short-cherry signal might be related to inappropriate processing of the Brp-short fragment after disassembling from the AZ[9]. Among other tested AZ proteins, fluorescently tagged DLiprin-α or *Drosophila* Rim Binding Protein (DRBP) constructs display a reduction in number of puncta and a clear delocalization in LL. In contrast, fluorescently tagged Dsyd-1 or Cacophony (Cac) do not display an increased cytoplasmic signal even after LL (**Figure 4G**). Thus, measuring systematically whether the signal becomes cytoplasmic might be of relevance to understand the processing of AZ proteins.

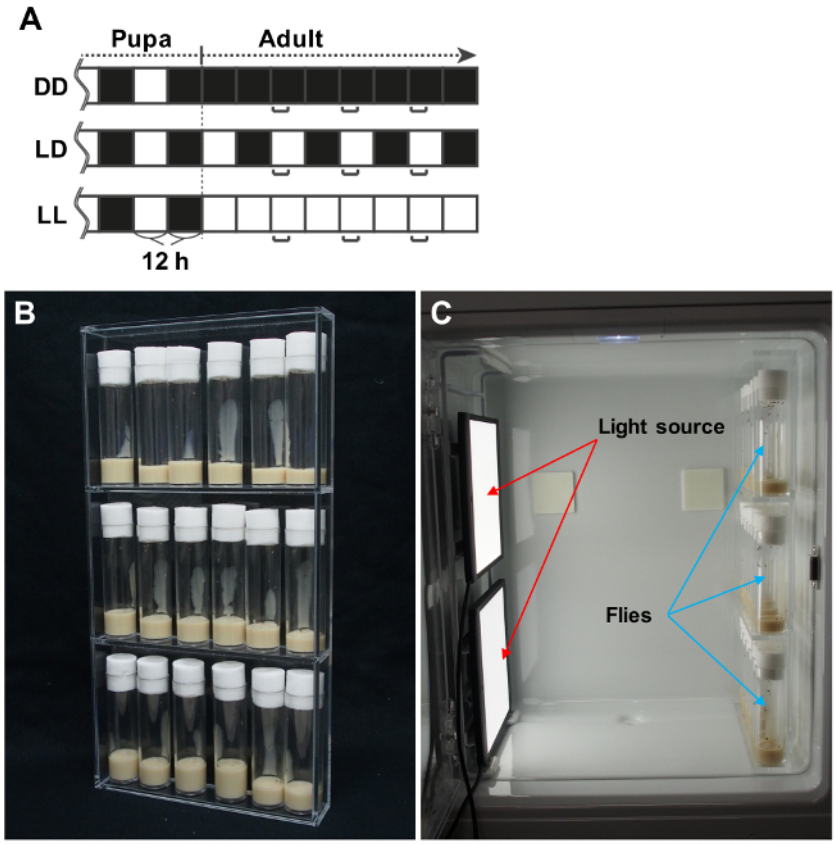


**Figure 1: Preparation of Conditions for Exposure to Defined Light Intensity. (A)** Light exposure protocols after eclosion. DD, continuous darkness; LD, 12 h light/12 h dark; LL, constant exposure to light. Fly brains were dissected at the times indicated in the brackets (Adapted from a previous publication[9]). **(B)** Vials are aligned in a customized acrylic transparent rack. **(C)** The acrylic rack and two LED panels are put in a small incubator and adjusted to expose the flies to a light intensity of 1,000 lux. Please click here to view a larger version of this figure.

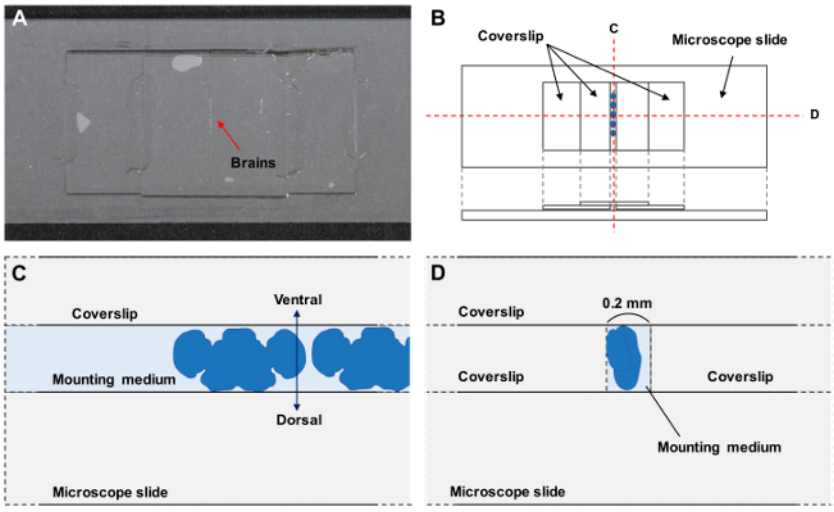


**Figure 2: Preparation of the Specimen. (A)** Whole mounted brain preparations. **(B - D)** Schematic drawing of the preparations. **(C, D)** Cross-sections of the preparations. The ventral side of the brains is up **(C)** between coverslips **(D)**. Please click here to view a larger version of this figure.

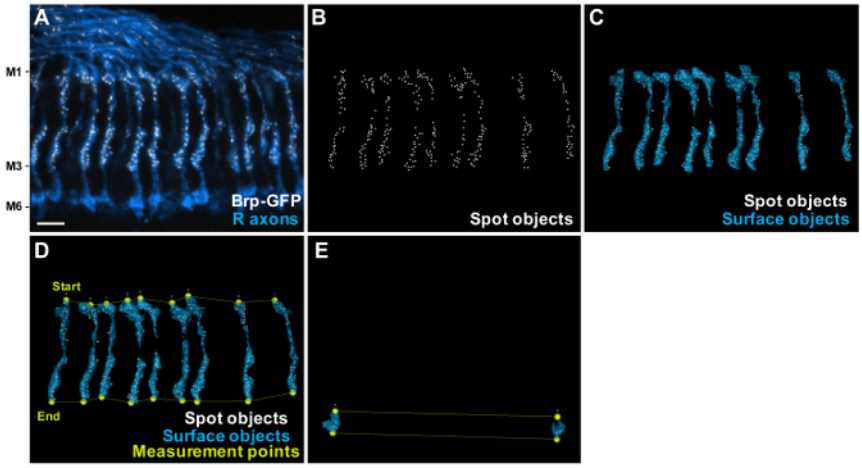


**Figure 3: Generation of the Spots, Surface Objects and Measurement Points. (A)** Projection of a confocal stack through the medulla layers M1 - M6, showing R8s Brp-GFP puncta (white) generated with STaR[15] using *sens-flp* recombinase. Anti-Chaoptin (blue) highlights the R7 and R8 photoreceptor axons. Scale bar, 5 µm. **(B)** Identification of Brp-GFP puncta by the spot detection module for each R8 axon terminal. **(C)** Detected axon regions ("Surface objects", blue) and spot regions ("Spot objects", white) for measuring the delocalization level of Brp-GFP in R8 axons. **(D)** The start-points and end-points are manually set with "measurement point" function to define each axon's orientation in 3D space and to define a coordinate system onto which the Brp-GFP spot are projected. **(E)** The surface objects, spots, start-points and end-points for two R7 axon terminals at M6 layer that do not include R8 are generated to subtract the background signal of the GFP channel. Please click here to view a larger version of this figure.

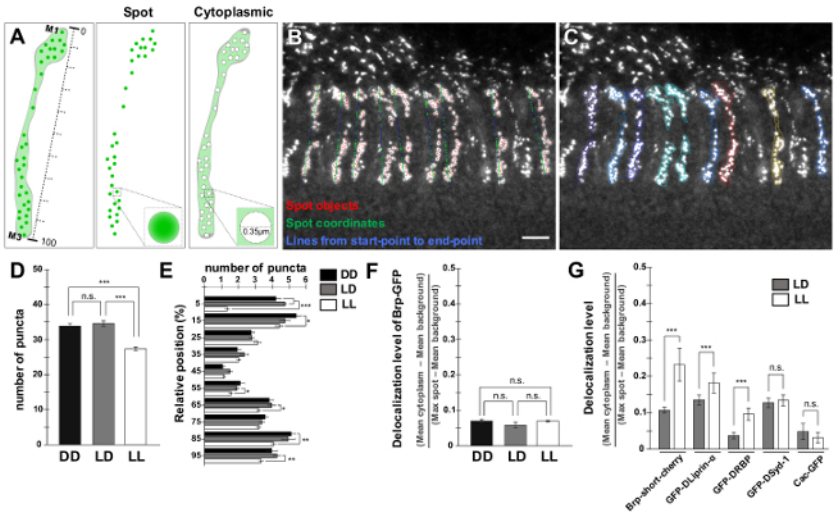


**Figure 4: Quantification of the Number, Distribution and Delocalization Level of Brp-GFP Puncta. (A)** Schematic drawing of the procedure utilized to measure the level of delocalized Brp-GFP signal in R8. The Brp-GFP puncta are identified and two areas are defined around them: the "spot" area and the "cytoplasmic" area. The line connecting start- and end-points is subdivided in 10 partitions. (**B, C**) Output from the customized image analysis software plugin written in a multi-paradigm numerical computing environment. Each Brp-GFP punctum coordinate is projected to a line representing the neuron from start-point to end-point **(B)**. Scale bar, 5 µm. The Brp-GFP puncta are identified and two areas are defined around them: the "spot" area and the "cytoplasmic" area **(C)**, as schematized in **(A)**. **(D - F)** Bar graphs comparing the total number of puncta **(D)**, their distribution **(E)** and the delocalization level of Brp-GFP per R8 axon **(F)** in DD (83 axons/7 brains), LD (107 axons/5 brains) and LL (226 axons/15 brains). **(G)** Bar graphs comparing the delocalization level of Brp-short-cherry in LD (74 axons/7 brains) and LL (70 axons/5 brains), GFP-DLiprin-α in LD (67 axons/7 brains) and LL (52 axons/6 brains), GFP-DRBP in LD (70 axons/7 brains) and LL (83 axons/6 brains), GFP-Dsyd-1 in LD (48 axons/5 brains) and LL (69 axons/7 brains), and Cac-GFP in LD (31 axons/5 brains) and LL (27 axons/5 brains). ***$p < 0.0001$, **$p < 0.001$, *$p < 0.05$, n.s. $p > 0.05$; unpaired t test with Welch's correction two-tailed. Error bar shows standard error of the mean. The schematic drawing in **(A)** and the data in **(D)**, **(E)** and **(G)** are adapted from a previous publication[9]. Please click here to view a larger version of this figure.

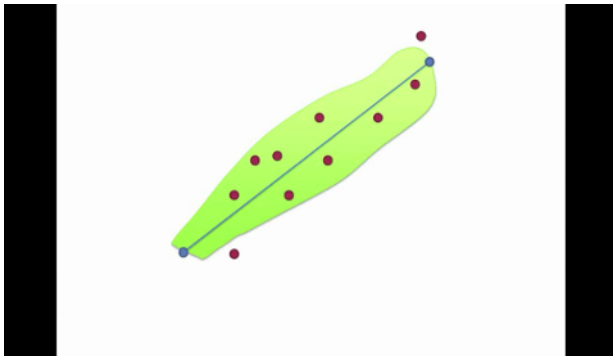

**Supplemental Video: Description of the Data Processing Performed with the Imaris Plugin "Synapse Trafo".** Discussion of data processing. This video contains a short lecture to illustrate the coordinate transformation and data processing steps performed by the Imaris plugin "synapse_trafo". Please click here to view this video. (Right-click to download.)

## Discussion

In this study, we showed how to prepare the light conditions to expose flies to an equal light intensity. We quantified not only the number of a synaptic marker puncta but could also spatially resolve the density of synapses along axons and measure the delocalization level of the marker protein in cytoplasmic areas. These three assessments allow us to evaluate the details of synaptic dynamics at single neuron level in different environmental conditions. Our protocol can be adapted to different synaptic proteins but also to any data that contains punctate signals.

A critical step within the protocol is the mounting of the brains. *Drosophila* photoreceptors project their axons to the second optic ganglion medulla. Each photoreceptor axon can be scanned straightforwardly if the mounted brains were correctly placed on a microscope slide. The correct mounting also makes the selection of photoreceptors with the image analysis software functions easier. Each photoreceptor region has to be selected manually for counting the number and delocalization level of puncta. The start- and end-points are also selected manually. These preparations require a relatively long time until one can proceed to the quantification. The advantage of R8 axons is that they are unbranched and each R8 axon is separate. A simple isolated neuron such as this one is recommended for these applications since it is necessary to define the exact area of the neuron. Additionally, this helps to get rid of nonspecific puncta and surfaces derived from other neurons. A limitation in this approach, however, is the depth of the z projection. The signal intensity of puncta gets less in deeper layers of the z stack. Preparing transparent brains by tissue-clearing methods such a SeeDB2[29] might help to overcome this limitation and allow imaging of a clear punctate signal even deeper in the brain.

Our protocol can potentially be used for analyzing synaptic organization at a nano scale and with live imaging. Combining super-resolution imaging (*e.g.,* stimulated emission depletion (STED) microscopy, stochastic optical reconstruction microscopy (STORM), photo activated localization microscopy (PALM), structured illumination microscopy (SIM) *etc.*) with theoretical modeling has advanced our understanding of the structure and molecular dynamics of synapses. For instance, the nanoscopic organization of Brp was evaluated at a single-molecular resolution with super-resolution imaging by direct STORM (*d*STORM) at the *Drosophila* NMJ[30]. Our protocol was adapted for quantification of dynamics of a single active zone molecule at a presynaptic active zone and of a single postsynaptic receptor at a postsynaptic zone to further understand how synapses are regulated at a mechanistic level. Moreover, our protocol could be used to visualize molecular movement at synapses in living animals. In fact, Brp-GFP can be visualized without relying on immunostaining. Thus, presynaptic development in R8 axons has been imaged in live animals with two-photon microscopy[15]. It is possible to track the punctate signal of active zone components in living animals by detecting and analyzing spots at different time points since the surfaces and positions of specific neurons are defined in our protocol.

## Disclosures

The authors have nothing to disclose.

## Acknowledgements

We are grateful to T. Stürner for helpful corrections, discussions and comments on the manuscript; S.L. Zipursky for providing fly stocks; M Schölling for performing image processing. Part of the image analysis was performed at A. Kakita's lab. This work was supported by Alexander von Humboldt Foundation and JSPS Fellowships for Research Abroad (A.S.), JSPS Fellows (S.H.-S.), Grant-In- Aid for Start-up (24800024), on Innovative Areas (25110713), Mochida, Takeda, Inamori, Daiichi-Sankyo, Toray Foundations (T.S.), DZNE core funding (G.T.) and DZNE Light Microscopy Facility (C.M.).

## References

1. Alabi, A. A., & Tsien, R. W. Synaptic Vesicle Pools and Dynamics. *Cold Spring Harbor Perspectives in Biology.* **4** (8) (2012).
2. Couteaux, R., & Pecot-Dechavassine, M. [Synaptic vesicles and pouches at the level of "active zones" of the neuromuscular junction]. *C R Acad Sci Hebd Seances Acad Sci D.* **271** (25), 2346-2349 (1970).
3. Schoch, S., & Gundelfinger, E. D. Molecular organization of the presynaptic active zone. *Cell and Tissue Research.* **326** (2), 379-391 (2006).
4. Sudhof, T. C. The Presynaptic Active Zone. *Neuron.* **75** (1), 11-25 (2012).

 

5. Owald, D., & Sigrist, S. J. Assembling the presynaptic active zone. *Curr Opin Neurobiol.* **19** (3), 311-318 (2009).
6. Lazarevic, V., Schone, C., Heine, M., Gundelfinger, E. D., & Fejtova, A. Extensive remodeling of the presynaptic cytomatrix upon homeostatic adaptation to network activity silencing. *J Neurosci.* **31** (28), 10189-10200 (2011).
7. Matz, J., Gilyan, A., Kolar, A., McCarvill, T., & Krueger, S. R. Rapid structural alterations of the active zone lead to sustained changes in neurotransmitter release. *Proc Natl Acad Sci U S A.* **107** (19), 8836-8841 (2010).
8. Spangler, S. A. *et al.* Liprin-alpha2 promotes the presynaptic recruitment and turnover of RIM1/CASK to facilitate synaptic transmission. *J Cell Biol.* **201** (6), 915-928 (2013).
9. Sugie, A. *et al.* Molecular Remodeling of the Presynaptic Active Zone of Drosophila Photoreceptors via Activity-Dependent Feedback. *Neuron.* **86** (3), 711-725 (2015).
10. Sigrist, S. J., & Schmitz, D. Structural and functional plasticity of the cytoplasmic active zone. *Curr Opin Neurobiol.* **21** (1), 144-150 (2011).
11. Kittel, R. J. *et al.* Active zone assembly and synaptic release. *Biochem Soc Trans.* **34** (Pt 5), 939-941 (2006).
12. Kittel, R. J. *et al.* Bruchpilot promotes active zone assembly, Ca2+ channel clustering, and vesicle release. *Science.* **312** (5776), 1051-1054 (2006).
13. Hallermann, S. *et al.* Naked dense bodies provoke depression. *J Neurosci.* **30** (43), 14340-14345 (2010).
14. Wagh, D. A. *et al.* Bruchpilot, a protein with homology to ELKS/CAST, is required for structural integrity and function of synaptic active zones in Drosophila. *Neuron.* **49** (6), 833-844 (2006).
15. Chen, Y. *et al.* Cell-type-specific labeling of synapses in vivo through synaptic tagging with recombination. *Neuron.* **81** (2), 280-293 (2014).
16. Andlauer, T. F., & Sigrist, S. J. Quantitative analysis of Drosophila larval neuromuscular junction morphology. *Cold Spring Harb Protoc.* **2012** (4), 490-493 (2012).
17. Ippolito, D. M., & Eroglu, C. Quantifying synapses: an immunocytochemistry-based assay to quantify synapse number. *J Vis Exp.* (45) (2010).
18. Schmitz, S. K. *et al.* Automated analysis of neuronal morphology, synapse number and synaptic recruitment. *J Neurosci Methods.* **195** (2), 185-193 (2011).
19. Danielson, E., & Lee, S. H. SynPAnal: software for rapid quantification of the density and intensity of protein puncta from fluorescence microscopy images of neurons. *PLoS One.* **9** (12), e115298 (2014).
20. Sanders, J., Singh, A., Sterne, G., Ye, B., & Zhou, J. Learning-guided automatic three dimensional synapse quantification for drosophila neurons. *BMC Bioinformatics.* **16** 177 (2015).
21. Peng, H., Ruan, Z., Atasoy, D., & Sternson, S. Automatic reconstruction of 3D neuron structures using a graph-augmented deformable model. *Bioinformatics.* **26** (12), i38-46 (2010).
22. Sturt, B. L., & Bamber, B. A. Automated quantification of synaptic fluorescence in C. elegans. *J Vis Exp.* (66) (2012).
23. Kremer, M. C. *et al.* Structural long-term changes at mushroom body input synapses. *Curr Biol.* **20** (21), 1938-1944 (2010).
24. Mosca, T. J., & Luo, L. Synaptic organization of the Drosophila antennal lobe and its regulation by the Teneurins. *Elife.* **3** e03726 (2014).
25. Wu, J. S., & Luo, L. A protocol for dissecting Drosophila melanogaster brains for live imaging or immunostaining. *Nat Protoc.* **1** (4), 2110-2115 (2006).
26. Fischbach, K. F., & Dittrich, A. P. M. The Optic Lobe of Drosophila-Melanogaster .1. A Golgi Analysis of Wild-Type Structure. *Cell and Tissue Research.* **258** (3), 441-475 (1989).
27. Berger-Muller, S. *et al.* Assessing the role of cell-surface molecules in central synaptogenesis in the Drosophila visual system. *PLoS One.* **8** (12), e83732 (2013).
28. Fouquet, W. *et al.* Maturation of active zone assembly by Drosophila Bruchpilot. *J Cell Biol.* **186** (1), 129-145 (2009).
29. Ke, M. T. *et al.* Super-Resolution Mapping of Neuronal Circuitry With an Index-Optimized Clearing Agent. *Cell Rep.* **14** (11), 2718-2732 (2016).
30. Ehmann, N. *et al.* Quantitative super-resolution imaging of Bruchpilot distinguishes active zone states. *Nat Commun.* **5** 4650 (2014).


 